

Disruption Prevention Using Rotating Resonant Magnetic Perturbation on J-TEXT

Da Li¹, Qingquan. Yu², Yonghua Ding^{1*}, Nengchao Wang^{1*}, Feiran Hu¹, Ruo Jia¹, Lai Peng¹, Bo Rao¹, Qiming Hu³, Hai Jin⁴, Mao Li¹, Lizhi Zhu¹, Zhuo Huang¹, Zebao Song¹, Song Zhou¹, Jianchao Li⁵, Ying He¹, Qi Zhang¹, Wei Zhang¹, Jiaolong Dong¹, Dongliang Han¹, Wei Zheng¹, Abba Alhaji Bala^{1,6}, Kexun Yu¹, Y. Liang^{1,7} and the J-TEXT team[†]

¹International Joint Research Laboratory of Magnetic Confinement Fusion and Plasma Physics, State Key Laboratory of Advanced Electromagnetic Engineering and Technology, School of Electrical and Electronic Engineering, Huazhong University of Science and Technology, Wuhan, 430074, China

²Max-Planck-Institut für Plasmaphysik, 85748 Garching, Germany

³Princeton Plasma Physics Laboratory, Princeton NJ 08543-0451, USA

⁴College of Electrical and Information Engineering, Lanzhou University of Technology, Lanzhou, China.

⁵Advanced Energy Research Center, Shenzhen University, Shenzhen, China

⁶Department of Physics, Federal University Dutse, Jigawa, Nigeria

⁷Forschungszentrum Jülich GmbH, Institut für Energie-und Klimaforschung-Plasmaphysik, 52425 Jülich, Germany

Corresponding Author:

Yonghua Ding, yhding@hust.edu.cn

Nengchao Wang, wangnc@hust.edu.cn

Abstract

Plasma major disruption is one of the most critical issues to be solved for a tokamak fusion reactor. Experiments to prevent mode locking and subsequent disruptions have been carried out on J-TEXT tokamak using rotating resonant magnetic perturbations (RMPs). The tearing modes, to be locked and to lead to disruptions without applying RMPs, can be accelerated by rotating RMPs to the RMP frequency. As the result, the mode locking and subsequent disruptions are delayed or prevented. The effects of RMP amplitude and frequency on disruption prevention have been investigated.

* Author to whom any correspondence should be addressed.

[†] See the author list of “Y. Liang *et al* 2019 Overview of the Recent Experimental Research on the J-TEXT Tokamak, *Nucl. Fusion* **59** 112016”

Keywords: disruption, mode locking, disruption prevention, resonant magnetic perturbation, tearing mode, J-TEXT

1. Introduction

During tokamak major disruptions[1], the rapid and complete loss of the thermal and magnetic energy generates high thermal and electromagnetic loads on the vessel and internal components, having highly damaging effect on the machine. Therefore, disruptions have to be prevented or mitigated for a fusion reactor. In experiments disruptions occur in different cases, e.g. in the discharges with a low edge safety factor, [2], too high plasma density or fraction of impurities[3], vertical displacement event (VDE)[4], and others[1]. The locked tearing mode, formed from the mode locking or error field penetration, is one of the major reasons for disruptions. On DIII-D, it is found that the modes with poloidal/toroidal mode numbers $m/n = 2/1$ are the most detrimental to plasma confinement and often lead to disruptions [5, 6]. The main root cause of disruptions on JET is due to the locking of (neoclassical) tearing modes [7, 8]. Active control of the locked mode is an important issue for disruption prevention[9, 10].

One possible way to prevent disruptions as well as to stabilize (neoclassical) tearing modes is using localized electron cyclotron current drive (ECCD)[11] as shown in experiments on ASDEX-U[12], FTU[13], DIII-D[14], JFT-2M[15] and TEXTOR[16]. To be effective, ECCD should be radially well aligned with the island[17] and applied before mode locking for preventing disruptions [11, 13]. Recent simulation result however showed that due to plasma density perturbations, a factor of 2 – 4 broadening in the wave absorption profile is expected for ITER, indicating a lower driven current density at the resonant surface and a corresponding higher wave power required for NTM stabilization[18]. On the TEXTOR tokamak, the disruptive mode locking was prevented by injecting low power NBI in the last phase of the slowing-down process[19]. Resonant magnetic perturbation (RMP) could steer the O-point of the magnetic island to the wave deposition region to increase the stabilizing efficiency, and the locked mode is suppressed as found in numerical modelling and experiments [20, 21].

Another possible way to prevent the locked mode is to drive the mode rotation by apply rotating RMPs. In the DIII-D high β_N operations ($\beta_N \sim 2.5$), the neoclassical tearing mode (NTM) was excited and led to disruptions, and RMPs were used to keep the mode to rotate at 17 Hz to prevent disruption[22].

The effect of RMPs on tearing modes has been studied before in J-TEXT, and the acceleration of tearing mode rotation has been found when applying high frequency rotating RMP[23, 24]. In addition,

driving a tearing mode locked to a static RMP to rotate again by rotating RMP has been tested[25, 26], in which the mode amplitude was relatively small, and the discharges were in the safe operation region, being far away from the disruption limit.

When the discharge becomes highly unstable with large amplitude tearing mode, however, it is not clear yet whether rotating RMPs can prevent or delay the mode locking and subsequent disruption. To learn this, experiments have been carried out on J-TEXT tokamak by using rotating RMPs of a few kilohertz to prevent the locked modes and disruptions. In this paper, the corresponding experimental results are reported. The experiments have been carried out in the regime with low edge safety factor q_a (from 3 to 2.3). In this regime the plasma becomes highly unstable to the tearing mode, and large amplitude tearing mode and mode locking usually occur, followed by disruption in 5 ~ 20 ms. Triggered by a mode locking warning system, the rotating RMP is applied before mode locking to maintain the mode rotation, to prevent mode locking and subsequent disruption. It is found that the RMP with a higher frequency and a moderate amplitude has the best performance for preventing disruptions.

In the following Section 2 the experimental setup is described, including the target plasma and the rotating RMP system. The experimental results are presented in Section 3. Finally, Section 4 gives the discussion and conclusion.

2. Experimental setup

J-TEXT[27] is a circular cross-section tokamak with the major radius $R_0 = 105$ cm (at magnetic axis) and minor radius $a = 25.5$ cm in our experiments. The $m/n = 2/1$ tearing mode usually appears in the operation regime with a sufficiently large plasma current I_p . By ramping up the I_p to decrease the edge safety factor q_a , the $2/1$ tearing mode grows and is then locked when the mode amplitude is large enough, causing the major disruption.

Fig. 1 displays a typical example of disruptions in this case. The blue line in Fig. 1(c) is the perturbed poloidal magnetic field generated by the tearing mode, measured by a toroidal magnetic probe array located at -45° from low field side midplane. The mode frequency is calculated from the time derivative of the phase of magnetic perturbations. When I_p is ramped up from 180 kA ($q_a = 3$) towards 230 kA ($q_a = 2.3$) within 150 ms (Fig. 1 (a)), the frequency of the tearing mode (f_{TM} , blue line in Fig. 1(c)) decreases as the mode amplitude ($\delta B_{\theta^{n=1}}$, red line in Fig. 1 (c)) increases, where $\delta B_{\theta^{n=1}}$ is the perturbed magnetic field of $n = 1$ component. This seems to be caused by the braking torques by the resistive wall, T_{rw} [28], which is proportional to the mode frequency and the square of the mode amplitude. When the mode amplitude was larger than a certain value, the mode frequency sharply

decreases. With the decreasing of tearing mode rotating frequency, the influence of T_{rw} becomes weaker, while the braking torque caused by the error field could eventually cause mode locking [23, 29]. When the mode is locked at 0.342 s, a minor thermal quench occurs shown by the electron cyclotron emission (ECE) signal at $(R-R_0) = -17$ cm at the midplane (Fig. 1 (d)), where R is the major radius. The major thermal and current quench, i.e. disruption, occurred shortly afterwards. This discharge is selected as the target scenario for our study on disruption prevention.

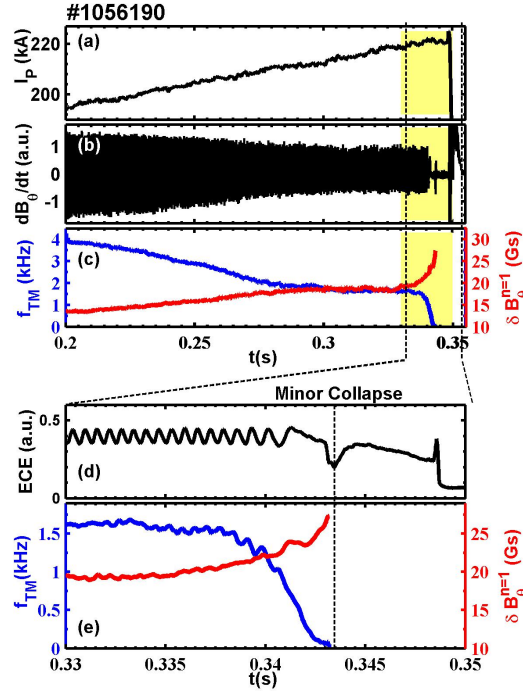


Fig. 1 A typical locked mode induced disruption during the ramp up of I_p . From top to the bottom, the time evolution of (a) I_p , (b) Mirnov signal, (c) frequency (blue line) and perturbed poloidal magnetic field of $n=1$ component (red line). The data around the disruption are displayed in (d) from electron cyclotron emission (ECE) signal at $(R-R_0) = -17$ cm (radial distance from the magnetic axis at midplane) and (e) mode frequency (blue line) and amplitude (red line). With increasing the I_p , the tearing mode amplitude increases, the mode locking and the disruption follow several millisecond later.

On J-TEXT, rotating RMPs are generated by 12 in-vessel saddle coils (3 rows \times 4 columns \times 1 turn)[30]. The RMP spectrum is chosen to have a large 2/1 component about 0.5 Gs/kA[30], as shown in figure 2(a). Two power supplies feed alternating current into the coils[31]. Recently, the AC power supplies were modified to allow a fast current ramp-up rate, and the AC current can reach its maximum 2.5 kA within 5ms to allow timely application of rotating RMPs. The dependence of RMP amplitude on its frequency at the plasma edge $r = a = 26.5$ cm, calculated in vacuum condition, is shown in figure 2(b).

Due to the short distance between RMP coils and vacuum vessel, the eddy current is generated by rotating RMP in vacuum vessel, which reduces the RMP amplitude at the plasma edge. The RMP amplitude is decreased by about 2/3 with increasing the RMP frequency from zero to hundreds Hz, and it only slightly decays from 1 to 5 kHz.

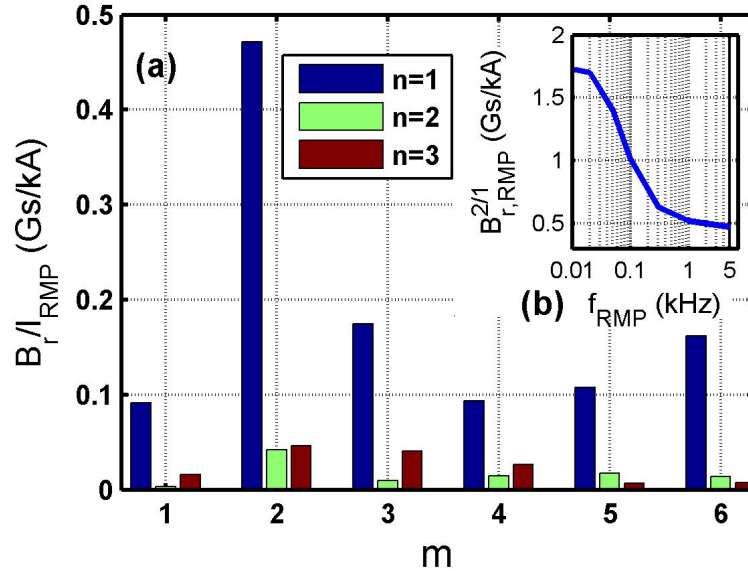


Fig. 2 (a) The spectrum of rotating RMPs at the plasma edge ($r = a = 26.5$ cm) for the toroidal mode number $n=1-3$ and the poloidal mode number $m=1-6$. (b) The amplitude of the radial $m/n = 2/1$ magnetic perturbation as a function of its frequency at $r = a$.

A mode locking warning system has been developed, measuring the instantaneous mode frequency to predict the mode locking [32]. Triggered by the warning system, the rotating RMP is applied around 7 ~ 20 ms before mode locking in experiments.

3. Experimental results

An example of preventing the disruption induced by locked mode is shown in Fig. 3. The rotating RMP of 3 kHz is applied in shot 1056200 before mode locking. The RMP frequency is higher than the original tearing mode frequency, ~2 kHz, before applying RMPs. With the RMP coil current $I_{RMP} = 1.5$ kA, the mode frequency is accelerated to the RMP frequency due to the electromagnetic torque applied from rotating RMPs. The mode amplitude is slightly suppressed around 0.335s and maintained at relatively lower level by the RMP in the plasma current flattop with $I_p = 230$ kA ($q_a = 2.3$). The disruption is prevented until the current ramp-down phase. While in the referenced discharge without

applying RMPs (#1056190), the mode amplitude increases during the ramp up phase of I_p , and the mode locking and disruption occur at a lower value of I_p (higher value of q_a). It is seen that the rotating RMP can prevent mode locking and the following disruption when applied before mode locking.

Although the rotating RMP is still turned-on during the I_p ramp down phase, the tearing mode grows up and causes disruption in this phase (shown by the red lines in Fig. 3). This is similar to the disruption observed in the current ramp down phase of the ITER baseline scenario in DIII-D[33]. Theoretical study proposed that the gradient of plasma current density was increased around the resonant surface during the I_p ramp down phase, and the tearing mode instability parameter, Δ' , was increased[34], causing the disruption. If so, the disruption during this phase can be prevented by a slower decrease of the plasma current, which is not the subject of our study presented here.

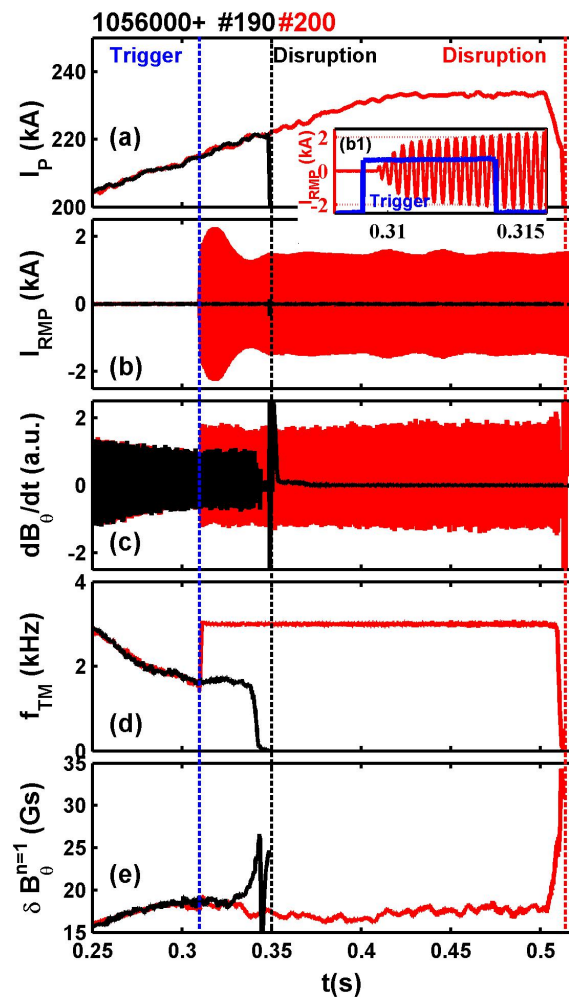


Fig. 3 Prevention of disruption by rotating RMP (3 kHz/ 1.5 kA, red), compared to a discharge without RMP which disrupted during the I_p ramp-up phase (black). From top to bottom, the time evolution of I_p (a), RMP coil current (b), Mirnov signal (c), the frequencies of tearing mode (d) and the perturbed poloidal magnetic field of $n = 1$ component (e). The blue vertical dashed line indicates the triggering time of rotating RMP generated by the

warning system. The rotating RMP accelerated the tearing mode rotation and prevented the disruption. The discharge was maintained until the current ramp-down phase.

To learn the optimal parameters of rotating RMP for preventing mode locking, rotating RMPs of different frequency and amplitude were tested in experiments.

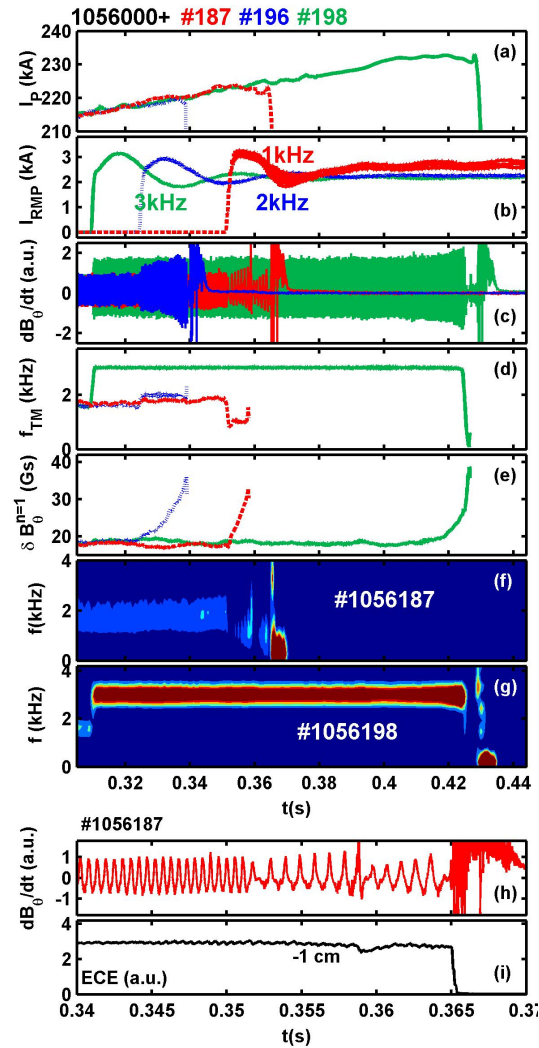


Fig. 4 Comparison of the impacts of rotating RMPs with 3 different frequencies, 1 kHz (#1056187, red dashed), 2 kHz (#1056192, blue dotted line) and 3 kHz (#1056198, green line). The RMP coil current are all about 2 kA. The time evolution of I_p (a), the amplitude of rotating RMP coil current (b), the signals of magnetic probe (c), tearing mode frequency (d), perturbed magnet field of $n = 1$ component (e) and the spectrogram of 1 kHz case (#1056187 (f) and 3 kHz case (#1056198 (g)). For the 1 kHz case right before disruption, the signals of magnetic probes (h) and the electron cyclotron emission at $(R-R_0) = -1$ cm (radial distance from the magnetic axis at midplane) (i) are also shown. The rotating RMP with higher frequency has a better effect on disruption prevention.

By applying different frequencies of RMPs, the results are shown in Fig. 4 with about the same RMP coil current, 2 kA. The original frequency of the tearing mode is around 2 kHz before applying the RMP. The rotating RMP of 3 kHz accelerates the mode rotation to the RMP frequency (green curves), and the discharge continues until the edge safety factor reaches $q_a = 2.3$. The lower frequency RMPs (2 kHz and 1 kHz) are not so effective for preventing the disruption. The RMP of 1 kHz decreases the tearing mode frequency, as shown by the red curve in Fig. 2 (d). After the mode is locked to the rotating RMP, its amplitude increases, as seen from Fig. 3 (e). Comparing the ECE signal at $(R-R_0) = -1$ cm (Fig 4(i)) with the magnetic probe signal (Fig 4 (h)), it is seen that the disruption occurs even before the mode frequency drops to zero. By applying the 2 kHz rotating RMP (blue line in Fig. 4), the disruption occurs soon similar to the 1 kHz case. It is seen from figure 4 that the natural mode frequency depends on the its radial location, which in turn depends on the q_a value. The decreasing q_a leads to a slightly higher natural mode frequency as shown the red curve in figure 4 (d).

Due to the difference in the time evolution of mode frequencies in different discharges, the rotating RMP is not triggered at the same time in these experiments. However, the applying time of rotating RMP has little influence on the results when it is applied before mode locking.

To further study the effect of 2 kHz rotating RMP, experiments have been carried out with different RMP coil current, $I_{\text{RMP}} = 1.7$ kA and 2 kA. With a smaller RMP coil current, $I_{\text{RMP}} = 1.7$ kA, the results are shown by the blue curve in figure 5. The mode is first locked to the RMP frequency, but the mode amplitude increases later during the increase of the plasma current. The ECE signal at $(R-R_0) = -1$ cm (Fig. 5 (g)) indicates that the mode frequency decreases towards zero before the disruption, and the electromagnetic torque generated by rotating RMP is not large enough to maintain the mode rotation at the RMP frequency. The case with a slightly larger RMP coil current, 2 kA (red), is worse than the 1.7 kA case. The mode amplitude increases after the mode is locked to the RMP frequency, and the mode frequency also decreases towards zero before the disruption. As the torque applied by rotating RMPs, T_{rmp} , is linearly proportional to the mode amplitude, while T_{rw} is proportional to the square of the mode amplitude, T_{rw} can be larger than T_{rmp} for a sufficiently large mode amplitude and slow down the mode rotation. It is seen that the mode amplitude is important in preventing the disruption by rotating RMPs. Only with the 3 kHz rotating RMP, the mode amplitude is maintained at relatively lower level for a long time period, as shown in figure 4, so that it is better for disruption prevention and is used in the following investigation.

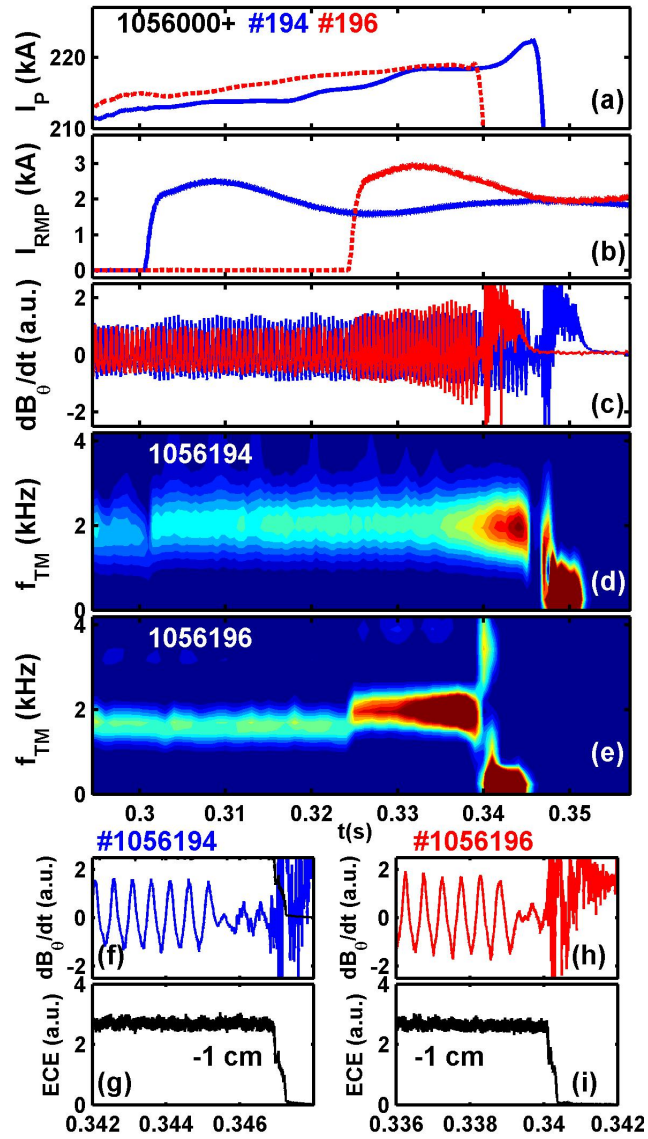


Fig. 5 Comparison of the impacts of rotating RMPs on mode locking with $I_{RMP} = 1.7$ kA (#1056194, blue line) and 2 kA (#1056196, red line). The RMP frequency are 2 kHz for both cases. The time evolution of I_P (a), the amplitude of rotating RMP coil current (b), spectrogram of the signals of magnetic probe for the 1.7 kA case (#1056194 (d)) and 2 kA case (#1056196 (e)), the Mirnov signal (f) / (h) and the electron cyclotron emission (ECE) signal at $(R-R_0) = -1$ cm (the radial distance from the magnetic axis at midplane) (g) / (i) for the 1.7 kA / 2 kA case right before disruption.

Fig. 6 shows the impact of RMP amplitude on the disruption prevention with the rotating RMPs of 3 kHz. The discharge #1056190 (black line) was the reference case without RMP. The RMP with the coil current $I_{RMP} = 2$ kA was applied in discharge #1056198 (green), which accelerates the mode rotation to the RMP frequency, and the minimum edge safety factor of 2.3 ($I_P = 230$ kA) is reached, but the mode amplitude increases later and trigger the disruption. By applying a moderate RMP ($I_{RMP} = 1.5$ kA,

#1056200, red), the mode amplitude is smaller than that of the 2 kA case, and the disruption was prevented until the I_P ramp down phase. For a too weak RMP ($I_{RMP} = 0.6$ kA, blue), the mode can't be accelerated to the RMP frequency, and the disruption occurred at about the same time as that in the reference case.

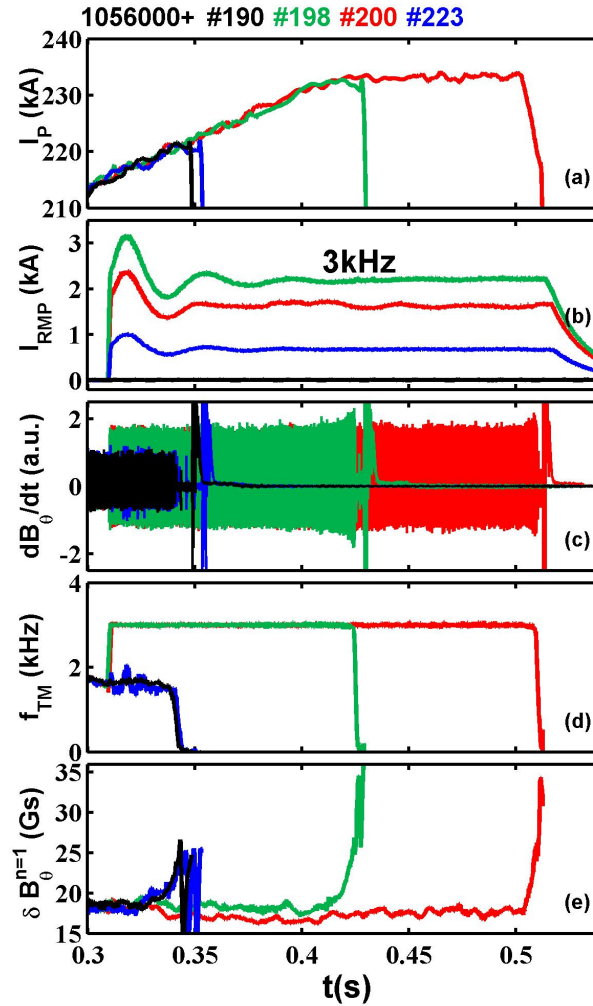


Fig. 6 Comparison of the impacts of rotating RMPs on mode locking with $I_{RMP} = 0$ kA (#1056190, black), 0.6 kA (#1056233, blue), 1.8 kA (#1056200, red) and 2.2 kA (#1056198, green). The RMP frequency is 3 kHz for all cases. The time evolution of I_P (a), the amplitude of RMP coil current (b), the signals of magnetic probe (c), mode frequency (d) and perturbed magnet field of $n = 1$ component (e). The rotating RMP with appropriate amplitude could prevent the disruption.

The dependence of the minimum q_a reached in experiments on the RMP amplitude is shown in Fig. 7. For the green points in the red square box, the q_a is achieved at the plasma current flattop, although the disruption occurs later during the current ramp-down phase. For others points, it is the minimum q_a

at which the discharge disrupts. Slower rotating RMPs of 1 kHz (red triangles) and of 2 kHz (blue stars) have little effect on the minimum q_a achieved comparing with the case of no RMP (black circle points). For the faster rotating RMP of 3 kHz (green squares), a too weak RMP can not change the tearing mode frequency as seen in figure 6, and the disruption occurs at about the same q_a as that without applying RMP, showing a lower threshold of RMP amplitude required to overcome the braking torques and to accelerate mode rotation to the RMP frequency. On the other hand, the mode amplitude increases with the RMP amplitude after the mode is locked to the rotating RMP. Once the rotating RMP amplitude is large enough to lock the tearing mode, a further increase in RMP amplitude would increase the mode amplitude as well as the minimum q_a that can be reached. The optimal RMP amplitude for the disruption prevention should neither be too small nor too large. With the RMP coil current in the range from 1 kA to 1.5 kA in our experiments, the discharges are maintained at $q_a = 2.3$ until the ramp down phase of plasma current. For a constant RMP frequency of 3kHz, the RMP amplitude at $r = a$ inside the vessel is linearly proportional to the RMP coil current.

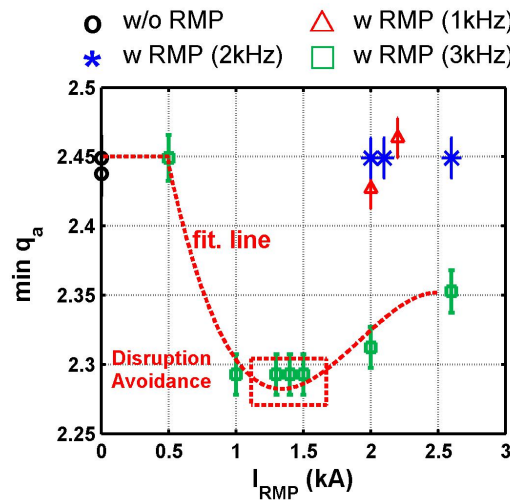


Fig. 7 The dependence of the minimum q_a reached in experiments on rotating RMPs amplitude, measured by the RMP coil current. The red triangles, blue stars and green squares are for the rotating RMP of 1 kHz, 2 kHz and 3 kHz, respectively. The error bar is marked on the figure. The slower rotating RMPs of 1 kHz and 2 kHz have little effect comparing to that without RMP (black circles). The rotating RMPs of 3 kHz prevent the disruption when the RMP coil current is in the range 1 kA - 1.5 kA. For the green points in the red square box, the q_a was achieved at the plasma current flattop, although the disruption occurs later during the current ramp-down phase. For other points, it is the minimum q_a at which the discharge disrupts.

4. Discussion and conclusion

To prevent or delay disruptions caused by mode locking, rotating RMPs of 3kHz are found to be much better than the lower frequency RMPs (1 kHz and 2 kHz) in our experiments. Although the mode frequency can be locked to the RMP frequency for all cases after applying RMPs, the mode amplitude increases later and causes disruptions for the lower frequency cases. The mode amplitude is at a relatively lower level for the 3kHz case, so that the disruption is significantly delayed or prevented. This is possibly due to the higher RMP frequency than the original mode frequency before applying RMPs. A faster mode rotation could decrease the destabilizing effect from mode coupling to other mode, e.g. the $m/n=1/1$ mode. It is not clear yet if the tearing mode amplitude can be further suppressed by RMPs of an even high frequency ($>3\text{kHz}$). The feedback control of the RMP amplitude would allow to optimize the disruption prevention by rotating RMPs in the future experiments.

Once the tearing mode is locked by the wall and error field, however, it is not possible to rotate the locked mode again by our rotating RMPs system. An example is shown in figure 8. After applying the rotating RMP of 1 kHz, only a small oscillation in the mode phase is observed, but it is much less than $\pi/2$, the predicted threshold for mode unlocking [28,29]. The disruption occurs similar to the case without applying RMPs. For preventing disruptions in our experiments, the rotating RMP should be applied before a large drop of mode frequency such that the full locking process has not started, as expected from existing theoretical and experimental results [10,19,28,29]. When the mode amplitude is sufficiently large, the braking torque generated by the resistive wall (proportional to the square of the mode amplitude)[28] could be large than that from rotating RMPs (proportional to the mode amplitude) [28,29].

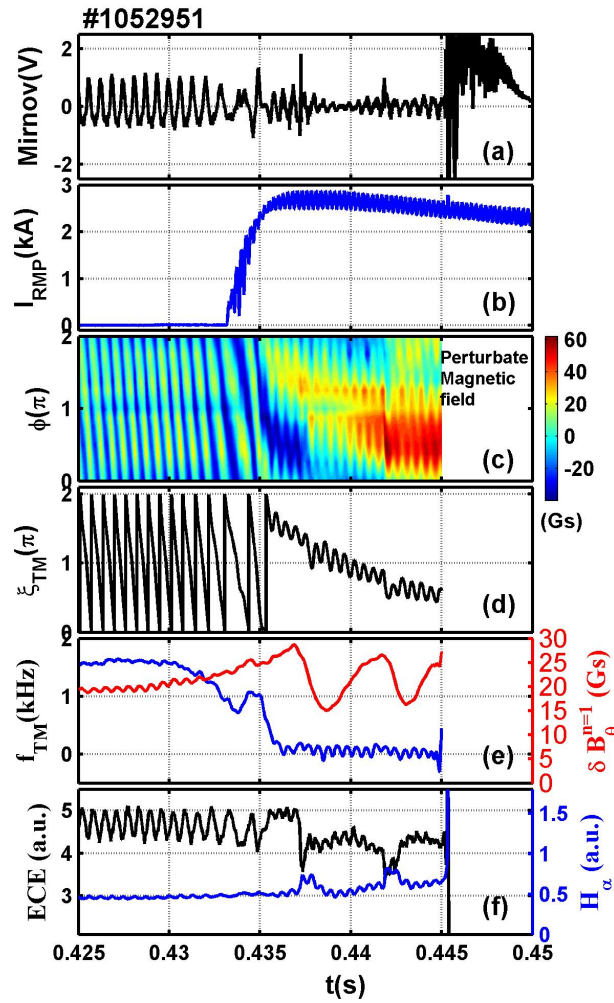


Fig. 8 Rotating RMP is applied after mode locking. The time evolution of magnetic probe signal (a), RMP coil current amplitude (b), contour of perturbed magnetic field generate by tearing mode (c), the phase of locked mode (d), perturbed magnet field of $n = 1$ component (red lines in (e)) and frequency (blue lines in (e)), the electron cyclotron emission (ECE) signal at $(R-R_0) = -13.5$ cm at the midplane (black line in (f)) and the H_α signal at edge (blue line in (f)).

For a fusion reactor like ITER, the plasma rotation velocity is expected to be much lower than that in existing tokamaks due to low torque input, being more easily subjected to mode locking [20]. The mode frequency could be in the level of diamagnetic drift frequency. Rotating RMPs of a sufficiently high frequency will be able to speed up the mode rotation and to delay or prevent mode locking and subsequent disruption, similar to the experimental results shown in this paper. \

In summary, preventing and delaying the mode locking and subsequent disruptions by using rotating RMP have been achieved on J-TEXT for the plasma operation in the low q_a regime ($q_a = 2.3$). With the RMP of 3kHz (higher than natural mode frequency) and appropriate amplitude, this q_a value is achieved

at the plasma current flattop. Rotating RMPs of sufficiently high frequency and moderate amplitude are more effective for this purpose, suggesting a possible method for delaying or preventing the disruptions caused by locked mode in a fusion reactor.

Acknowledgements

This work is supported by the National MCF Energy R&D Program of China under Grant No. 2018YFE0309100 and the National Key R&D Program of China under Grant No. 2017YFE0301100, National Magnetic Confinement Fusion Science Program of China Contract No. 2015GB111001, the National Natural Science Foundation of China (Contract No. 11275080, 11405068 and 11505069).

References

- [1] Wesson J, Gill R, Hugon M, *et al.* Disruptions in JET. *Nuclear Fusion*, 1989, 29: 641
- [2] R. Sweeney, W. Choi, R. J. La Haye, S. Mao, K. E. J. Olofsson and F. A. Volpe *Nuclear Fusion* **57**, (2017)
- [3] Zhang Y, Pautasso G, Kardaun O, *et al.* Prediction of disruptions on ASDEX Upgrade using discriminant analysis. *Nuclear Fusion*, 2011, 51: 063039
- [4] Gruber O, Lackner K, Pautasso G, *et al.* Vertical displacement events and halo currents. *Plasma Physics & Controlled Fusion*, 1993, 35: B191-B204
- [5] Sweeney R, Choi W, Austin M, *et al.* Relationship between locked modes and thermal quenches in DIII-D. *Nuclear Fusion*, 2018, 58: 056022
- [6] Sweeney R, Choi W, La Haye R, *et al.* Statistical analysis of $m/n=2/1$ locked and quasi-stationary modes with rotating precursors at DIII-D. *Nuclear Fusion*, 2016, 57: 016019
- [7] de Vries P C, Johnson M F, Segui I. Statistical analysis of disruptions in JET. *Nuclear Fusion*, 2009, 49: 055011
- [8] de Vries P C, Johnson M F, Alper B, *et al.* Survey of disruption causes at JET. *Nuclear Fusion*, 2011, 51: 053018
- [9] De Vries P C, Pautasso G, Nardon E, *et al.* Scaling of the MHD perturbation amplitude required to trigger a disruption and predictions for ITER. *Nuclear Fusion*, 2016, 56: 026007
- [10] E.J. Strait, J.L. Barr, M. Baruzzo *et al.* Progress in disruption prevention for ITER. *Nuclear Fusion*, 2019, 59: 112012
- [11] Wang X, Yu Q, Zhang X, *et al.* Numerical modelling on stabilizing large magnetic island by RF current for disruption avoidance. *Nuclear Fusion*, 2017, 58: 016045
- [12] Esposito B, Granucci G, Maraschek M, *et al.* Avoidance of disruptions at high β_N in ASDEX Upgrade with off-axis ECRH. *Nuclear Fusion*, 2011, 51: 083051
- [13] Esposito B, Granucci G, Smeulders P, *et al.* Disruption avoidance in the Frascati Tokamak Upgrade by means of magnetohydrodynamic mode stabilization using electron-cyclotron-resonance heating. *Physical review letters*, 2008, 100: 045006
- [14] Petty C C, Haye R J L, Luce T C, *et al.* Complete suppression of $m/n=2/1$ neoclassical tearing mode using electron cyclotron current drive in DIII-D. *Nuclear Fusion*, 2004, 44: 243-251
- [15] Hoshino K, Mori M, Yamamoto T, *et al.* Avoidance of $q_a=3$ disruption by electron cyclotron heating in the JFT-2M tokamak. *Physical review letters*, 1992, 69: 2208
- [16] Classen I, Westerhof E, Domier C, *et al.* Effect of heating on the suppression of tearing modes in tokamaks. *Physical review letters*, 2007, 98: 035001
- [17] Maraschek M, Gantenbein G, Yu Q, *et al.* Enhancement of the stabilization efficiency of a neoclassical magnetic island by modulated electron cyclotron current drive in the ASDEX Upgrade tokamak. *Physical review letters*, 2007, 98: 025005
- [18] Snicker A, Poli E, Maj O, *et al.* The effect of density fluctuations on electron cyclotron beam broadening and implications for ITER. *Nuclear Fusion*, 2017, 58: 016002
- [19] P. de Vries, *et al.* MHD-mode stabilization by plasma rotation in TEXTOR *Plasma Phys. Control, Fusion* **38** (1997) 467
- [20] Yu Q, Günter S. Locking of neoclassical tearing modes by error fields and its stabilization by RF current. *Nuclear Fusion*, 2008, 48: 065004
- [21] Volpe F, Hyatt A, La Haye R J, *et al.* Avoiding tokamak disruptions by applying static magnetic fields that align locked modes with stabilizing wave-driven currents. *Physical review letters*, 2015, 115: 175002
- [22] Okabayashi M, Zanca P, Strait E, *et al.* Avoidance of tearing mode locking with electro-magnetic torque introduced by feedback-based mode rotation control in DIII-D and RFX-mod. *Nuclear Fusion*, 2017, 57: 016035
- [23] Hu Q, Rao B, Yu Q, *et al.* Understanding the effect of resonant magnetic perturbations on tearing mode dynamics. *Physics of Plasmas*, 2013, 20: 92502-92511
- [24] Rao B, Ding Y H, Hu Q M, *et al.* First observation of rotation acceleration of magnetic island by using rotating resonant magnetic

- perturbation on the J-TEXT tokamak. *Plasma Physics & Controlled Fusion*, 2013, 55: 122001
- [25] Jin H, Hu Q, Wang N, *et al.* Locked mode unlocking by rotating resonant magnetic perturbations in J-TEXT tokamak. *Plasma Physics & Controlled Fusion*, 2015, 57: 104007
- [26] Wang N, Rao B, Hu Q, *et al.* Plasma response to rotating resonant magnetic perturbations with a locked mode in the J-TEXT tokamak. *Nuclear Fusion*, 2019, 59: 026010
- [27] Liang Y, Wang N, Ding Y H, *et al.* Overview of the recent experimental research on the J-TEXT tokamak. *Nuclear Fusion*, 2019,
- [28] Nave M, Wesson J. Mode locking in tokamaks. *Nuclear Fusion*, 1990, 30: 2575
- [29] Fitzpatrick R. Interaction of tearing modes with external structures in cylindrical geometry (plasma). *Nuclear Fusion*, 1993, 33: 1049
- [30] Rao B, Wang G, Ding Y H, *et al.* Introduction to resonant magnetic perturbation coils of the J-TEXT Tokamak. *Fusion Engineering & Design*, 2014, 89: 378-384
- [31] Yi B, Ding Y H, Zhang M, *et al.* Design of the power system for dynamic resonant magnetic perturbation coils on the J-TEXT tokamak. *Fusion Engineering and Design*, 2013, 88: 1528-1532
- [32] Rao B, Li D, Hu F R, *et al.* Fast island phase identification for tearing mode feedback control on J-TEXT tokamak. *Review of Scientific Instruments*, 2016, 87: 1153-1159
- [33] Turco F, Luce T, Solomon W, *et al.* The causes of the disruptive tearing instabilities of the ITER Baseline Scenario in DIII-D. *Nuclear Fusion*, 2018, 58: 106043
- [34] Hegna C, Callen J D. Stability of tearing modes in tokamak plasmas. *Physics of plasmas*, 1994, 1: 2308-2318